Temperature Evolution of Excitonic Absorptions in $Cd_{1-x}Zn_xTe$ Materials

Manuel A. Quijada and Ross Henry

Goddard Space Flight Center, Code 551, Greenbelt, MD 20771, USA

ABSTRACT

The studies consist of measuring the frequency dependent transmittance (T) and reflectance (R) above and below the optical band-gap in the UV/Visible and infrared frequency ranges for $Cd_{1-x}Zn_xTe$ materials for x=0 and x=0.04. Measurements were also done in the temperature range from 5 to 300 K. The results show that the optical gap near 1.49 eV at 300 K increases to 1.62 eV at 5 K. Finally, we observe sharp absorption peaks near this gap energy at low temperatures. The close proximity of these peaks to the optical transition threshold suggests that they originate from the creation of bound electron-hole pairs or excitons. The decay of these excitonic absorptions may contribute to a photoluminescence and transient background response of these back-illuminated HgCdTe CCD detectors.

Keywords: Keywords: CdZnTe, UV/Vis infrared, transmittance, reflectance, semiconducting gap, photoluminescence, exciton

1. INTRODUCTION

The ternary compound $Cd_{1-x}Zn_xTe$ (CdZnTe) is a semiconducting alloy that is widely used as a base material for x-ray and infrared detectors. In particular, single crystals of CdZnTe wafers are the principal material on which HgCdTe epitaxial layers have been recently grown for the fabrication of infrared sensors on lattice matched CdZnTe substrate.[1] This has been possible due to recent advances through use of new detector growth technologies[2] which involve p/n double layer planar heterostructure arrays grown by Molecular Beam Epitaxy (MBE). This new technology offers very significant advantages as detectors in the 1–5 μm region over more conventional devices. Furthermore, these advances, along with those in lightweight mirror and adaptive optics technologies, have already revolutionized ground based infrared astronomy and now pave the way for the science program of space missions such as the James Webb Space Telescope (JWST) and the scheduled replacement of the Wide Field Camera 3 instrument on the Hubble Space Telescope (HST).

As shown in the diagram of Fig 1, the focal plane arrays developed using these technologies are backside illuminated. This means that the infrared light reaching the detector must first go through the CdZnTe substrate layer before it reaches the active layer in which it is to be absorbed. Hence, the detector performance will be influenced by the optical properties of the CdZnTe substrates on which the HgCdTe layers are grown.

Review of the literature[3] shows that most of the past studies on optical properties of $Cd_{1-x}Zn_xTe$ have been devoted to n–type and p–type doped CdTe with relatively high absorption coefficient ($\alpha > 1$ cm^{-1}) corresponding to high carrier density, while less has been reported on the optical properties of CdZnTe at low carrier density. It should be pointed out that doping the parent CdTe compound with small amounts of zinc is done with the purpose of better matching the coefficient of thermal expansion of CdZnTe to that of HgCdTe. In one room-temperature study,[4] it was found that the band-gap of a zinc-doped sample of $Cd_{1-x}Zn_xTe$ ($x \approx 0.1$) exhibits significant changes relative to that of a pure CdTe sample. At the same time, information about the temperature variation in the optical properties for samples with low zinc concentrations is very limited. This paper will address this deficiency by reporting temperature dependence in the optical constants for pure and a lightly Zn-doped samples $x \approx 0.04$ of the material $Cd_{1-x}Zn_xTe$. The importance of this can hardly be overstated since the space application of detector technologies mentioned above are meant to be used at temperatures much below 300 K and in some cases down to 30 K.

Send correspondence to M.A.Q. (E-mail: manuel.a.quijada@nasa.gov) Telephone: 1 301 286 3544

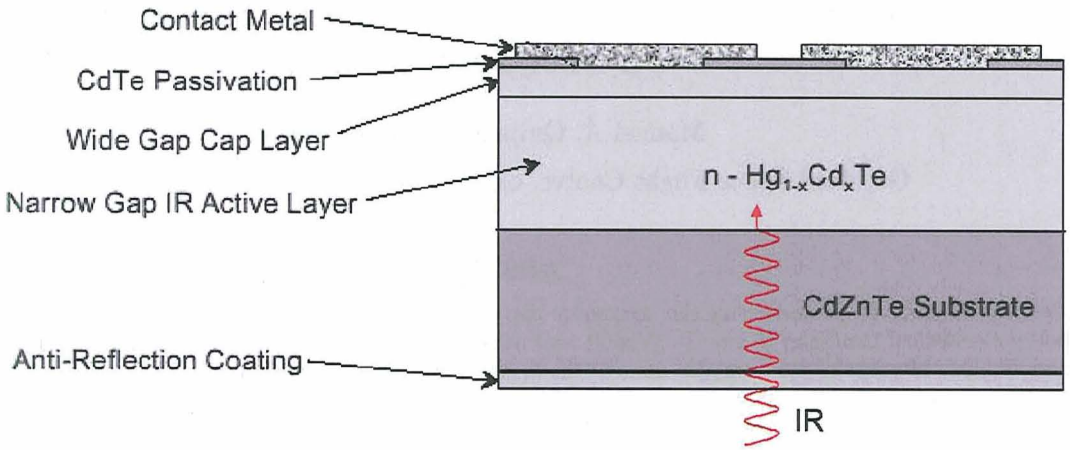

Figure 1. Cross-section view of a MBE grown HgCdTe photodiode. An n-type layer of HgCdTe is grown on a CdZnTe substrate, followed by a wide gap and passivation CTE layer to form the junction. Infrared flux is incident through the IR-transparent substrate.

The studies presented here consist of measuring the transmittance and reflectance at normal angle of incidence in the frequency range of 20 to 50,000 cm^{-1} (500$-$0.2 μm), and for temperatures in the 5$-$300 K range. In the IR range, where the sample is transparent (300$-$12500 cm^{-1}), the measured T and $\Re$ are used to derive the optical properties by solving the non-linear equations that relate the Fresnel coefficients of transmission and reflection to the sample optical constants. These solutions will yield the refractive index (n) and extinction coefficient (k) as a function of frequency and temperature.

In the frequency range where the sample transmittance is zero ($T(\omega) = 0$), we performed a Kramers-Kronig (KK) transformation analysis using the measured $\Re(\omega)$ in the phonon region and above the sample band gap. This was done for two reasons. First, this provided a self-consisting comparison to the dielectric function derived using the measured $T(\omega)$ and $\Re(\omega)$ using the Fresnel coefficients as described above. Secondly, the KK transformation of the specular reflectance allowed determination of the optical properties in the range where the sample was opaque.

The paper is organized as follows. First, we will present a description of the experimental set-up used in collecting the optical data. This include the optical spectrometer and the cryostat that allowed cooling the sample temperature down to 5 K. Next, we will present a brief characterization study carried out to determine the chemical composition of the samples used in these optical measurements. Next,we will present the experimental results, along with a a discussion of the changes that are seen in the dielectric constat in the semiconducting gap and the presence of excitonic features and the implications these will have for the HgCdTe detector performance. Finally, there will be some concluding remarks.

2. EXPERIMENTAL DETAILS

2.1 Spectral Measurements

The instruments used to obtain spectral scans of transmittance and reflectance of these CdZnTe samples were a combination of a Bruker IFS 113v fast-scan Fourier Transform spectrometer (FTIR), and a Perkin Elmer (PE Lambda 950) grating instrument. The FTIR instrument consists of a Genzel interferometer, whose principle of operation is similar to that of a Michelson interferometer. It comes equipped with three sources; a mercury arc, a glow-bar, and a tungsten lamp for spectral coverage in the far-IR and Mid-IR and visible regions respectively (20$-$20,000 cm^{-1}. There is a bolometer, room temperature DTGS, and Si diode detectors for each of those

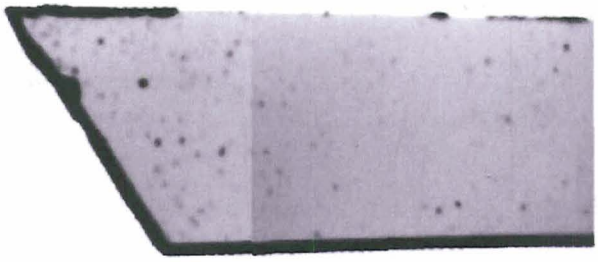

Figure 2. Infrared image of one CdZnTe substrate piece showing no evidence of area defects.

regions, and corresponding beamsplitters consisting of Mylar sheets of various thicknesses for the Far-IR range and a KBr and CaF_2 beamsplitters for the Mid-IR and NIR/visible regions respectively.

The PE Lambda 950 is a double-beam monochromator, ratio recording spectrometer that is used for coverage in the near-infrared/visible and ultraviolet spectral regions (3000−50,000 cm^{-1}). The light sources are a tungsten-halogen lamp for the NIR and VIS ranges, and a deuterium (D_2) lamp for the UV region. The detectors consist of a photomultiplier tube (PMT) for the UV-VIS and a PbS detector for the NIR.

Transmittance data, $T(\omega)$, for these samples were obtained by taking the ratio of the sample spectral transmission, at a normal angle of incidence, relative to the transmission of an empty hole. In the case of reflectance, $\Re(\omega)$, the spectral response of the light reflected off at 12° angle of incidence was taken relative the reflection of a reference gold sample. The resulting ratio of the sample to the reference mirror reflection was multiplied by the known reflectance of the gold mirror to obtain a properly normalized sample reflectance.

Cryogenic measurements of $T(\omega)$ and $\Re(\omega)$ in the temperature range of 5−300 K were done by mounting the sample at the tip of an Oxford Instruments continuous flow cryostat (Optistat CF). A flexible transfer line was used to flow liquid helium from a storage tank to the cryostat. The temperature of the sample was stabilized by using a temperature controller connected to a previously calibrated Si diode sensor and heating element attached to the tip of the cryostat. In this setup, the temperature of the sample could be lowered by increasing the flow of liquid helium and raised by applying a current to the heater element. During measurements, the sample holder and cryostat units were placed inside a shroud equipped with optical windows in the spectrometer sample chamber. The pressure inside this shroud was kept below 10^{-6} Torr to prevent the formation of ice in the cryostat or on the sample surface.

2.2 Chemical Analysis

Table 1. Chemical analysis results of two CdZnTe samples. Results of atomic composition are presented in %.

Sample 1	I	II	III	IV	Sample 2	I	II	III	IV
Zn	1.90	2.11	1.59	2.05	Zn	1.64	2.07	2.3	1.43
Cd	48.20	48.45	48.70	48.75	Cd	48.57	48.75	48.38	48.57
Te	49.90	49.43	49.70	49.20	Te	49.69	49.55	49.32	50.00

The CdZnTe samples used in this study are grown as boules using the Bridgeman Method and then sawn into slabs and polished. The chemical analysis consisted of a nondestructive energy dispersive x-ray spectrometer (EDS) in conjunction with a scanning electron microscope. There were a total of two samples with roughly equal area dimensions of $\approx$ 8×10 mm and thickness of 0.8 mm. Table 1 shows the results of a composition study of done on these CdZnTe samples. We looked at four different spots on each sample, with a spot size of 100 μm×100 μm in area. The differences seen in Zn content from spot to spot for a given sample are statistical variation due to the uncertainties in the measurement technique. Therefore, an average of these values suggest that the Zn content in each sample is around $x \simeq 0.04$.

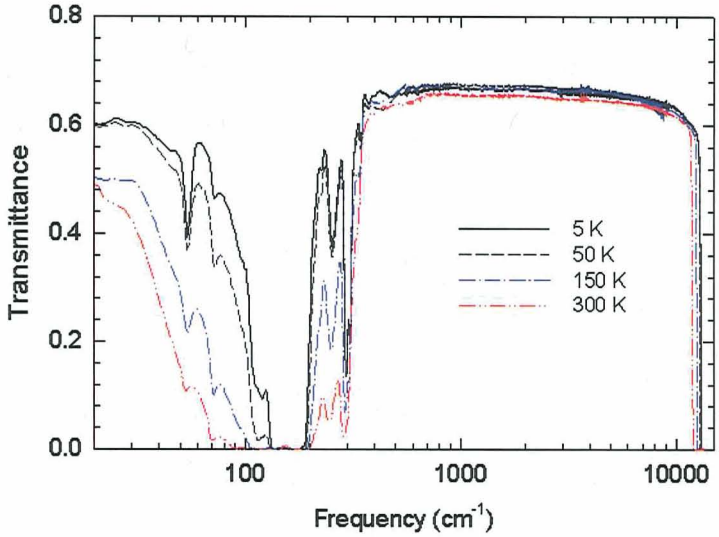

Figure 3. Temperature dependence of the transmittance of CdZnTe sample.

Figure 2 shows an infrared transmission image of one of the CdZnTe substrate wafers taken with an Inframetrics Model 600 IR radiometer. This camera operates in the 8–12 μm bandwidth and has a liquid nitrogen cooled (77 K) HgCdTe detector. The imaged CdZnTe showed no evidence of area defects (grain or twin boundaries). The image does reveal what appear to be tiny and dispersed Te inclusions (dark spots). Note that the image above is two separate images combined using a cut and paste and the linear feature is an artifact of this operation. Spot checks of the second CdZnTe sample considered in this study were also done and they showed the same apparent dispersed Te inclusions as shown in Fig. 2.

3. RESULTS AND DISCUSSION

3.1 Transmittance as Function of Temperature

Figure 3 displays the temperature variation of the optical transmittance, $T(\omega)$, for the CdZnTe sample. Several features are evident from this figure. First, the sample shows a transmission window below 100 cm^{-1} (100 μm) that increases at lower temperatures. This is indicative of the insulating nature of the sample. A few dips in $T(\omega)$ suggest the presence of some weak absorption features in this energy range. This is followed by a frequency band in the 100–200 cm^{-1} range where the sample becomes completely opaque. As it will be discussed later, this is due to the presence of IR active optical phonon in the Far-IR spectral region. Furthermore, the transmittance opens up to a constant value ($\simeq$ 65%) in the IR range (300–12,500 cm^{-1}), which includes the active wavelength range of the HgCdTe detectors (1–5 μm). Finally, the band-gap energy that is represented at the cut-off frequency of $T(\omega)$ in the high side of Fig. 3 increases as the temperature of the sample is reduced. This is shown more clearly in Fig. 4, where the gap starts at a value of $\sim$ 1.49 eV (12,000 cm^{-1}), and it increases linearly with decreasing temperature down to 100 K. The rate of decrease is reduced below this temperature reaching a value of 1.62 eV (13,000 cm^{-1}) at 5 K.

3.2 Reflectance as Function of Temperature

The corresponding near-normal $\Re(\omega)$ curves, which are complementary to the $T(\omega)$ discussed in Sec. 3.1 are shown in Fig. 5. There are two major observations to make here. The first one is that in the regions where the sample is transparent, the light reflected off the CdZnTe substrate contains front and back side contributions. This is illustrate by the fact that $\Re(\omega)$ shows enhanced values in those regions. Secondly, in the regions where the substrate is opaque, the reflectance is purely specular containing only a front-side component. A KK

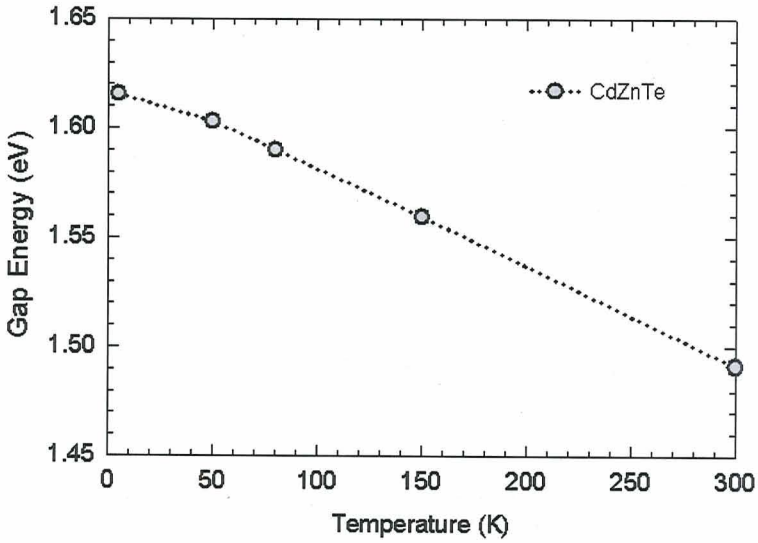

Figure 4. Temperature dependence of the transmittance edge or band gap of the CdZnTe sample.

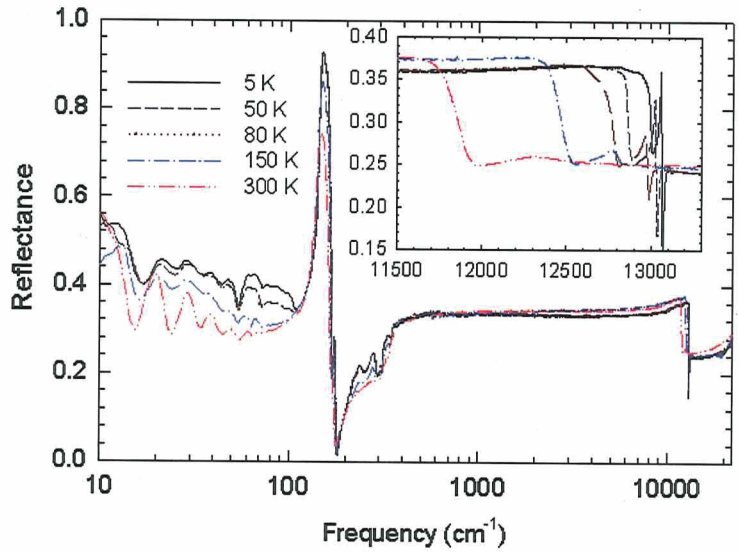

Figure 5. Temperature dependence of the transmittance of CdZnTe sample.

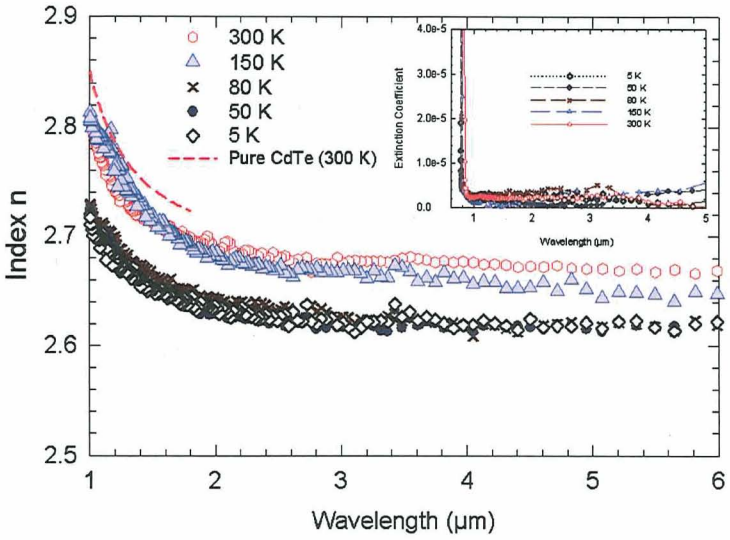

Figure 6. Refractive index, n, as function wavelength and temperature. For comparison, we show published 300 K data for a pure CdTe sample.[3] Inset: Extinction coefficient k.

transformation on the specular $\Re$ will yield information about the absorptive as well as the dispersive parts of the material optical properties. For these reasons, it is instructive to discuss the observed shapes of $\Re(\omega)$ in these opaque regions. For example, as discussed earlier in the far-IR region between 100 and 300 cm^{-1} where $T(\omega) = 0$, the $\Re(\omega)$ shown in Fig. 5 displays a derivative-like shape that suggests the presence of a strong optical phonon absorption.

Also, a closer look to the inset of Fig. 5 near the band-gap region suggests that the temperature dependence of the reflectance edge in $\Re(\omega)$ closely matches the behavior of the blue-edge cut-off of $T(\omega)$ of Fig. 4.

Finally, we notice some very sharp features more clearly seen in the inset of Fig. 5. These look like derivative-like peaks just below the band gap energy of CdZnTe. We also see that these peaks move to higher frequencies at lower temperatures along with the gap energy. As we will discuss later, this is evidence of excitonic absorptions that are frequently observed in direct band-gap semiconductors.[5]

3.3 Index of Refraction and Extinction Coefficient

We now turn our attention to using the data in Fig. 3 and Fig. 5 to determine the optical constants of the CdZnTe sample. This is done by using the equations derived in Appendix **??** and by solving for the refractive index n and the extinction coefficient k from the measured $T(\omega)$ and $\Re(\omega)$. Since it is impossible to directly invert these equations given that there are multiple roots, *i.e.*, multiple values of n and k that satisfy Eq. **??**, we solves these by employing a root-finding numerical solutions based on the secant and Mueller method.[6]

The results of these calculations are shown in Fig. 6 for n, while the inset of that figure shows the values for k. The results for n at 300 K show a 2 % reduction when compared to published room-temperature values for pure CdTe.[3] Furthermore, we observe almost no temperature dependence from 300 K to 150 K, but the data show an average 4 % reduction throughout the transparent wavelength range of CdZnTe at 80 K and lower temperatures.

Turning our attention to the inset Fig. 6, we see that as expected, the extinction coefficient is very small ($\sim 5 \times 10^{-6}$) in this region. Only near the gap energy does k start showing a substantial increase.

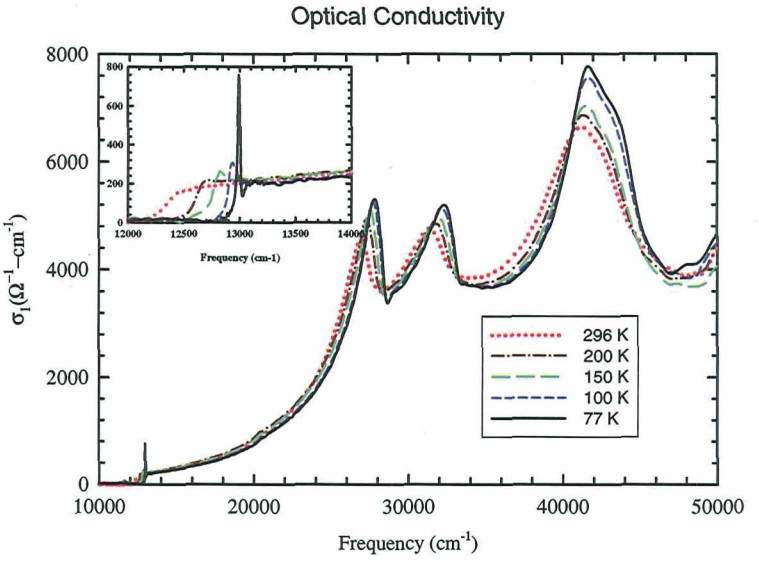

Figure 7. Frequency-dependent optical conductivity, $\sigma_1(\omega)$ in the 5−300K temperature range.

3.4 Optical conductivity: Evidence of Excitons

For energies above the band gap of CdZnTe, a KK analysis of the reflectance data shown in Fig. 5 was performed. The extrapolation procedure in the high-frequency end of the data was handled as described in Sect. ??. At the low end, we simply extrapolated the lowest measured value of $\Re$ to remain constant down to $\omega = 0$, as it is customary for insulators.

The results of the optical conductivity, $\sigma_1(\omega)$, derived from Eq. ?? are shown in Fig. 7. This figure shows that the onset of absorption in the CdZnTe samples moves to higher energies as the temperature of the sample is lowered. We also observe the presence of absorption peaks, whose positions in energy move along the temperature dependence of the band-gap energy. The strengths of these peaks grow in intensity at lower temperatures. That suggests they result from the creation of electron-hole pairs or exciton in this direct band-gap semiconductor.[5] Excitons are unstable with respect to radiative recombination in which the electron drops into the hole in the valence band. This leads to the emission of a photon or phonons.

The process of a photon emission will lead to a photoluminescence signal, as it has already been reported in the literature.[7] A possible consequence of such an emissive process in backside illuminated HgCdTe detectors could be elevated signal from substrate generated photons. The transient response signal in the detector would have a decay time proportional to the substrate exciton lifetime. This mechanism could explain recent measurements of backside illuminated HgCdTe detectors which report an elevated signal during proton irradiation.[8]

4. CONCLUSIONS

In conclusion, measurements of the optical properties for a $Cd_{0.96}Zn_{0.04}Te$ substrate that is used as a substrate layer to grow HgCdTe detectors shows an index value n in the transparent region that is 2% lower that the one measured on a pure CdTe sample. Further measurements of n show a weak temperature dependence from 300 to 150 K, followed by a 4 % reduction across the transparent region of CdZnTe at 80 K and lower temperatures.

Finally, results of the optical conductivity at energies just above the band-gap region show very sharp and narrow exciton peaks at low temperatures. These results could have implications for the performance of back illuminated CCD HgCdTe detectors, due to the fact that exciton decay may create an elevated background transient response, whose time response may be proportional to the exciton lifetime.

ACKNOWLEDGMENTS

We would like to thank Bradford Parker from the Materials Engineering Branch (Code 553, NASA-GSFC) for assistance in the chemical analysis study of these samples. Special thanks go the Jason Lynch a Virginia Tech summer inter for helping out during the cryogenic testing reported here. Finally, we would like to acknowledge useful discussion with Prof. Dennis Drew (University Maryland, College Park, MD) regarding the interpretation of optical data presented in this work.

REFERENCES

1. P. Norton, "HgCdTe infrared detectors," *Opto-Electronic Review* **10**, pp. 159–174, 2002.
2. D. N. Hall, "2048x2048 HgCdTe arrays for astronomy at visible and infrared wavelenghts (invited paper)," *in Proc. SPIE* **3356-1**, p. ???, 1998.
3. P. Klocek, *Handbook of Infrared Optical Materials*, Dekker Editor, New York, 1991.
4. H.W. Yao, J.C. Erickson, H.B. Barber, R.B. James, and H. Hermon, "Optical properties of $Cd_{0.9}Zn_{0.1}Te$ studied by variable angle spectroscopic ellipsometry between 0.75 and 6.24 ev," *Journal of Electronic Materials* **28**, pp. 760–771, 1999.
5. C. Kittel, *Introduction to Solid State Physics*, Addison-Wesley, New York, Chichester, Brisbane, Toronto, Singapore, 1986.
6. W.H. Press, B.P. Flannery, S.A. Teukolsky, and W.T. Vetterling, *Numercial Recipes*, Cambridge University Pres, New York, Australia, 1989.
7. S. Jain, *Photoluminescence study of cadmium zinc telluride*, Master Thesis, West Virginia University, Morgantown, West Virginia, 2001.
8. A. Waczynski, R.W. Marshall, R. Foltz, C.J. Marshall, R.A. Kimble, S.D. Johnson, G. Delo, A.M. Russel, Y. Wen, E.J. polidan, S. Reed, J.J. Yagelowich, and R.J. Hill, "Radiations effects in mercury cadmium telluride detectors," *in Proc. SPIE* **5902-25**, p. 122, 2005.